Malaysian Journal of Analytical Sciences (MJAS)
Published by Malaysian Analytical Sciences Society

DIRECT CATALYTIC CONVERSION OF CELLULOSE INTO FORMIC ACID BY SUPPORTED PHOSPHOTUNGSTIC ACID CATALYST

(Penukaran Terus Selulosa Kepada Asid Formik Menggunakan Pemangkin Asid Fosfotungstik yang Disokong)

Nor Liyana Zakira Zabidi Adil @ Zaibidai Adil, Farah Wahida Harun, Syaza Azhari, Lailatun Nazirah Ozair, Shikh Mohd Shahrul Nizan Shikh Zahari, Tengku Shafazila Tengku Saharuddin*

Faculty of Science and Technology,
Universiti Sains Islam Malaysia, Bandar Baru Nilai, 71800 Nilai, Negeri Sembilan

**Corresponding author: shafazila@usim.edu.my*

Received: 15 August 2021; Accepted: 11 January 2022; Published: 28 April 2022

Abstract

This study aims to prepare phosphotungstic acid supported on hydrotalcite (PTA-HT) for one-pot hydrothermal cellulose conversion into formic acid (FA). In this study, different percentages of PTA on HT (1, 5, 10, 15, 20, 25, and 33%) were prepared and the catalytic activity was observed for two different parameters such as time (1 to 5 hours) and reaction temperature (160 to 240 °C). The prepared catalysts were characterized using Fourier transform infrared (FTIR), X-ray powder diffraction (XRD), Brunauer-Emmet-Teller (BET) and field emission scanning electron microscopy-energy dispersive X-ray spectrometry (FESEM-EDX), while the production of FA was determined using ultra high-performance liquid chromatography (UHPLC). To avoid bias, raw PTA and calcined HT were compared with varying percentages of supported PTA. PTA-HT was successfully prepared through the impregnation method as confirmed by XRD, FTIR, BET and FESEM-EDX. According to the results, the optimum condition for cellulose conversion into formic acid was when 25% PTA-HT was applied at 220 °C for 4 hours, with a 30% cellulose conversion and 18 % FA yield. Due to the acidity and redox properties of PTA, it has been demonstrated that PTA-HT increased the catalytic activity by two-fold when compared to calcined HT alone (8%). The significance of this finding opens new suggestion of bifunctional catalyst in cellulose conversion into FA.

Keywords: catalyst, cellulose, formic acid, hydrothermal, phosphotungstic acid

Abstrak

Tujuan kajian ini adalah untuk menyediakan asid fosfotungstik yang disokong dengan oleh hidrotalsit (PTA-HT) bagi proses hidroterma penukaran selulosa kepada asid formik. Di dalam kajian ini, perbezaan peratus PTA ke atas HT (1, 5, 10, 15, 20, 25 dan 33%) telah disediakan dan aktiviti pemangkinan telah dijalankan terhadap dua parameter iaitu masa (1 jam hingga 5 jam) dan suhu (160 hingga 240 ℃). Pemangkin yang telah disediakan diperincikan menggunakan inframerah transformasi Fourier (FTIR), pembelauan sinar-X (XRD), Brunauer-Emmet-Teller (BET) and mikroskopi imbasan pancaran medan-spektrometri tenaga serakan sinar-X (FESEM-EDX) manakala asid formik yang terhasil ditentukan menggunakan kromatografi cecair berprestasi ultra tinggi (UHPLC). Bagi mengelakkan keputusan yang berat sebelah dalam kajian, PTA tulen dan HT yang dikalsin telah dibandingkan dengan perbezaan peratus PTA yang disokong. PTA-HT yang telah disediakan melalui kaedah

impregnasi dicirikan oleh XRD, FTIR, BET dan FESEM-EDX. Berdasarkan keputusan, keadaan yang paling optimum bagi penukaran selulosa kepada asid formik adalah apabila 25% PTA-HT digunakan pada 220 °C selama 4 jam dengan menghasilkan 30% penukaran selulosa dan 18% penghasilan asid formik. Oleh kerana ciri-ciri asid dan redoks yang dimiliki oleh PTA, keputusan kajian telah menunjukkan bahawa PTA yang disokong oleh HT meningkatkan aktiviti pemangkin sebanyak dua kali ganda berbanding HT yang telah dikalsin yang hanya menghasilkan 8% asid formik. Kepentingan kajian ini akan membuka cadangan baru terhadap penggunaan pemangkin dwifungsi dalam penukaran selulosa kepada asid formik.

Kata kunci: pemangkin, selulosa, asid formik, hidroterma, asid fosfotungstik

Introduction

Biomass is a great alternative for carbon sources in the production of platform chemicals as biomass originated from plants and animals [1]. Numbers of researches focused on forestry and agricultural residues as it is non-edible to address food competition issues such as wood [2], corncob waste [3] and rice husk [4]. Plant biomass is made up of three main constituents: cellulose, hemicellulose and lignin. Among these constituents, cellulose has the highest percentage and play important structural function for plant cell walls [5, 6]. Cellulose is a polymer that is highly crystalline due to rigid intermolecular bonds of hydrogen to hydroxyl group and oxygen with nearby glycosidic rings [7, 8]. Glycosidic bonds of cellulose causes difficulty in depolymerizing cellulose, which required highly reactive catalyst and rigorous experimental conditions. In converting cellulose, many techniques have been studied such as pretreatment of cellulose using ball-milling [9], addition of oxidant [10], Fenton reaction [11-13], hydrolysis [14, 15], ozonation [2] and oxidation [16]. A successful cellulose conversion provides production of important chemicals such as formic acid [17-19], lactic acid [20, 21], levulinic acid [22] and acetic acid [23]. Industries have been eyeing formic acid (FA) due to its nontoxicity, noncorrosive, easy handling and readily biodegradable qualities [24]. Formic acid is the most basic form of carboxylic acid and is commonly used as a byproduct in a variety of applications such as agriculture [25], cosmetics [26], textile [27] and pharmaceuticals [28].

Mineral acids such as hydrochloric acid, sulfuric acid and phosphoric acid have previously been used as acid catalysts for cellulose conversion due to their strong acidity and low cost, but these catalysts are highly corrosive [29-33]. Therefore, improvement had been made to convert cellulose using solid acid catalyst such as heteropoly acid [16], zirconia, zeolite and montmorillite [34]. The advantageous of using solid catalyst is that it is less corrosive, easier to handle, and separates the catalyst from the reaction medium. Among all catalysts, heteropoly acid (HPA) catalyst appears to be the most promising due to its strong Bronsted acidity and redox property [35] that able to hydrolyze and oxidize cellulose into FA. Nevertheless, drawbacks of homogenous HPA are low thermal stability, low surface area and easily soluble in polar solvent [35]. Supporting HPA on a suitable support is one way to heterogenized HPA, which can improve product yield, selectivity, and reduce HPA's drawbacks by providing more active sites and making it more porous [14, 22, 35, 36]. In addition, hydrotalcite (HT), a potential support material with a high surface area and basic properties that may aid in the catalytic conversion of cellulose, is one such material that has been widely used–in flame retardance, neutralizing additives, a base catalyst for cellulose conversion and adsorbent [37-40]. Therefore, in this work, cellulose conversion into FA by different percentages of PTA ($H_3PW_{12}O_4$) supported with HT ($Mg_6Al_2CO_3(_{16})\cdot 4H_2O$) were investigated to see the effects of temperature, time and PTA amount towards the production of FA.

Materials and Methods

Materials

All reagents were analytical grade and used without further purification such as hydrotalcite (Sigma-Aldrich), microcrystalline cellulose and ethanol 99.5% (Systerma) while formic acid 98-100% HPLC grade, tungstophsphoric acid hydrate, orthophosphoric acid and potassium dihydrogen phosphate were purchased from Merck.

Preparation of catalyst

The catalyst preparation starts with the reconstruction pathway in which commercial HT was calcined at 450 °C for 4 hours under nitrogen gas to remove carbonate ions. This step is to allow anions from raw PTA solution to enter into the empty interlayer region later [41]. The raw PTA was dissolved into deionized water to the desired amount (1, 5, 10, 15, 20, 25 and 33% by w/w%). Meanwhile, calcined HT was dissolved in another beaker. Subsequently, dissolved PTA was added dropwise into calcined HT solution. At this step, calcined HT will reconstruct into its original shape with new interlayer anions from PTA. This is because calcined HT regains its original structure when exposed to the aqueous solution [42]. Then, the mixture was stirred for 4 hours to ensure that PTA and calcined HT until both solutions were well-mixed. Lastly, the mixture was dried overnight to remove the water from the mixture forming a solid containing PTA and calcined HT.

Catalytic experiment

Cellulose conversion was conducted in a 100 mL hydrothermal reactor in which the contents of catalyst and cellulose fed were 0.1 g and 0.05 g respectively. Then, about 50 mL of deionized water was added. The reactor was tightened and placed inside an oven. Once reaction temperature and time were up, the cellulose conversion started. As soon as the required temperature and time were reached, the liquid product was filtered using a syringe filter and the solid residue was filtered using a vacuum pump. Cellulose conversion was calculated according to Equation 1. The concentration of FA was analyzed using the UHPLC system (1290 Infinity, Agilent Technologies) using Zorbax SB C18 column with an internal diameter of 21.2mm and 5µm particle size. The UHPLC system was connected with a DAD detector measuring at 210 nm. 10 mM phosphate buffer with pH adjusted to pH 2 was prepared, filtered and degassed. The concentration of FA from the sample was identified by comparing the retention times with standards. Standards calibration was used for FA quantification. The yield of FA was calculated using Equation 2 [43].

$$\text{Cellulose conversion} = \frac{\text{Cellulose fed} - (\text{Solid residue} - \text{Catalyst})}{\text{Cellulose fed}} \text{x} 100\% \quad (1)$$

$$\text{Formic acid yield} = \frac{\text{Liquid product}}{(\text{Stoichiometric coefficient FA from glucan})(\frac{\text{Cellulose fed}}{\text{Mass of glucan}})} \text{ x } 100 \quad (2)$$

Catalyst characterization

Nitrogen adsorption was done to differentiate specific surface area, pore size distribution and pore volume of PTA-HT, raw PTA, calcined HT and raw HT using Brunner-Emmet-Teller (BET) model 3 Flex Micromeritics. BET analysis started with degassing the sample to remove unwanted adsorbed molecules inside the sample pore. The thermal condition of degassing is prior to thermal gravimetric analysis to ensure that the sample was not destroyed during degassing. After degassing, the sample was placed inside the sample tube and liquid nitrogen was filled inside the dewar and placed below the sample tube for BET analysis. Then, phase characterization was carried out by X-ray diffraction (XRD) model Mini Flex 600, Rigaku with Cu Kα 1.54 (40 kV, 40 mA) X-ray radiation source at angle range 3^{θ} to 90^{θ}. In order to identify the crystalline phase compositions, the diffraction patterns were matched with Crystallography Open Database (COD). Chemical functional groups identification was carried out using Fourier Transform Infrared (FTIR) model Nicolet™ iS50 FTIR Spectrometer, Thermo Scientific. FTIR sample was grind using pestle and mortar until it become fine and thin. The sample analysis started after placing the sample onto the detector and background scanning was done. Then, surface morphology of sample was confirmed by Field Emission Scanning Electron Microscope (FESEM) model JSM-IT 800 FESEM, Joel with accelerating voltage 20 kV. Sample was coated with platinum using JEOL Smart Coater. The FESEM images were paired with Energy Dispersive X-ray Analysis (EDX) model Ultimax 45

Oxford to confirm the presence of elemental composition of each sample.

Results and Discussion

Catalytic activity

Three parameters were investigated to find the best conditions for FA production from cellulose using the PTA-HT catalyst: reaction time, temperature, and amount of PTA. The influence of reaction time towards FA production is displayed in Figure 1. To determine the best reaction time, the temperature and amount of PTA were kept constant at 180 ℃ and 5%, respectively. From the results, FA yield increased gradually from 0.08% to 0.22% between 1 to 3 hours of the reaction time. The value then increased slightly to 0.24% at 4 hours and remained constant until 5 hours. In the case of cellulose degradation, a longer reaction time allowed higher degradation rates ranging from 15% to 42% and does not achieve a plateau. From the result, it is observed that reaction condition for both cellulose degradation and FA yield at 180 ℃ is very mild although the reaction time varies from 1 hour to 5 hours. This can be seen when the reaction time was prolonged to 5 hours the cellulose degradation is slightly increased from 30 to 44% while FA yield remain constant as shown in Figure 1. Degradation of cellulose can be done independently without the presence of catalyst as reported in previous journal [44]. However, high temperature of water was required range 320 to 400 ℃ but cellulose was able to degrade into cellobiose, glucose and fructose [44]. Another study of cellulose degradation without presence of catalyst also observed the same trend where at 180℃ degradation products such as acids, furans and sugar were not detectable with only 12% cellulose converted [45]. Meanwhile, as shown in Figure 1, our experiment shows that at 180 ℃, cellulose degradation increases as reaction time prolonged and FA was detectable and reached a plateau at 4 hours reaction time. The production of FA which may cause by the presence of 5% PTA-HT that enhance cellulose degradation. This is because PTA contains tungsten ions and oxygen ions that does have an effect on hydrolysis and oxidation. Although hydrolysis mainly took place in a high temperature water medium, the production of the targeted product requires oxidation of cellulose where PTA provide additional oxygen located at bridging and terminal oxygen atom. However, the reaction time, water temperature and acidic strength of PTA was only able to hydrolyse cellulose but this condition is not enough to produce more FA. Hence, to improve this, we further with the next condition at 4 hours reaction time with the same amount of PTA to determine the suitable temperature and amount of PTA on HT catalyst.

Subsequently, the effect of reaction temperature on FA production was examined by varying the reaction temperature from 160 to 280 ℃. As illustrated in Figure 2, a noticeable increment can be seen towards cellulose degradation from 9% to nearly 50% with prolonged temperature. FA yield also showed better improvement with a maximum yield of 13.36% at 240 ℃. However, a very slight change in FA yield was observed between 220 ℃ (13.05 %) and 240 ℃ (13.36%). From the graph, the trend of FA yield started to decrease at 250 to 280 ℃ although cellulose degradation increases. The suggested mechanism pathway started with cellulose undergoes hydrolysis which form glucose [46]. The glucose further dehydrated into hydroxymethylfurfural (HMF) where later rehydrated into levulinic acid and decomposed into FA [47]. It is reasonable to speculate that higher temperature promotes degradation of cellulose as stated in [48] where cellulose can be degraded without the presence of acid at high temperature. However, previous journal [45] only highlighted the production of monosaccharides but our study proved that with the presence of PTA it enhances cellulose degradation route until FA was produced at suitable temperature. This occurs due to Brönsted acidity of PTA that highly protonate ions during reaction took place. Although, production of FA was a success, FA is an unstable compound which can easily decomposed into CO_2 [43][9]. Hence, selecting 220℃ as our reaction temperature is reasonable to avoid decomposition of FA.

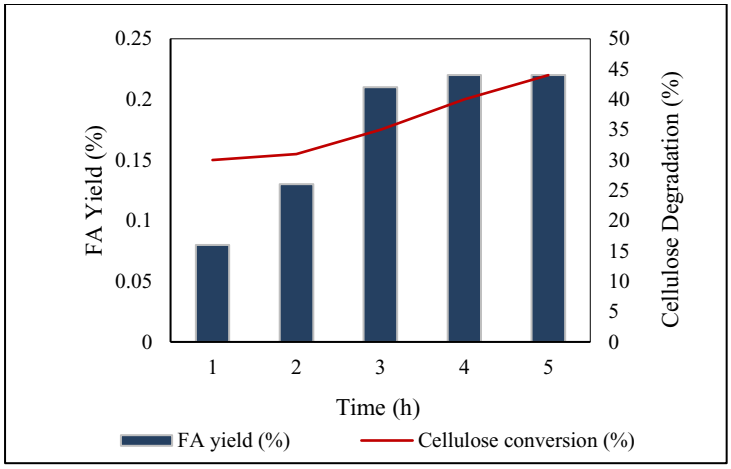

Figure 1. Effect of reaction time on cellulose conversion and FA yield by PTA-HT catalyst. Reaction condition: 0.05 g cellulose, 0.1 g PTA-HT, the temperature at 180 ℃ and PTA loading on HT is 5%

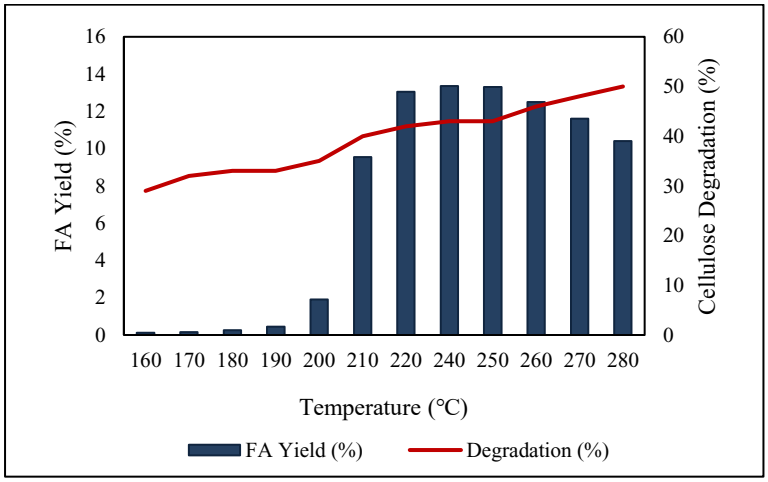

Figure 2. Effect of reaction temperature on cellulose conversion and FA yield by PTA-HT catalyst. Reaction condition: 0.05 g cellulose, 0.1 g PTA-HT, 5% PTA-HT and 4 hours reaction time

The influence of PTA amount supported on calcined HT was displayed in Figure 3. This investigation was compared with blank experiment where catalyst was not included during cellulose degradation. In Figure 3, although cellulose was degraded in blank experiment, FA yield was not obtained. However, other reactors that contained PTA-HT yielded FA. This phenomenon is possible to occur due to PTA criteria that is highly protonic acid which speed up the cellulose degradation [41]. Hence, FA can be obtained in 4 hours under 220 ℃ water temperature. A factor that allows hydrolysis to happen in blank experiment is when water medium is heated to high temperature but as observed our solid acid catalyst improves the hydrolysis rate and react further to form FA. Furthermore, the degradation rate in blank experiment was lesser as compared when PTA-HT was presence. The formation of FA occurred due to cascade reaction in which dehydration and rehydration took place before FA was formed. So as Brönsted acid was placed in the medium, hydrogen ions were highly dissociated which speed up dehydration of glucose into HMF which later

rehydrate into FA [44]. From our experiment, FA production depends on the acidic strength of our catalyst as FA yield increase with increasing amount of PTA but the FA yield was inconsistent. However, FA yield drops drastically to 0.08% when 33% of PTA-HT was placed in reaction medium while highest yield of FA (18%) was observed with 25% amount of PTA. To our surprise, calcined HT alone produce 8% FA which initially function as catalyst support.

Based on previous literature, calcined HT contains medium-strong Lewis basic O^{2+}-Mn^{n+} pairs and isolated O^{2-} as strong basic sites which promote production of FA compared with uncalcined HT that contain weak basic sites [49]. After cellulose was hydrolyze, glucose was not dehydrated into HMF instead isomerizes into fructose and retro-aldol forming glycolic acid. Then, dehydrated into lactic acid which later degraded into FA [50,51, 38]. From this, we understand that two possible routes occurred during FA production as illustrated in Scheme 1. PTA and HT when combined together consist of both acid and base sites. Having Brönsted acid feature increase degradation rate of cellulose while the basic site of calcined HT hindered decomposition of FA into carbon dioxide. 25 % PTA-HT was chosen to further investigate and characterize its properties in relation to the catalytic reaction. 25% PTA-HT was compared with calcined 25% PTA-HT to observe any difference in FA production. Cellulose degradation from calcined 25% PTA-HT was better than blank and calcined HT. The FA yield decreased drastically when PTA loading are more than 25%. This might happen due to leaching of PTA. Another similar study, compared uncalcined tungsten-based zirconia and calcined tungsten-based zirconia reported the same result [52]. From Figure 4, the UHPLC result shows the formation of FA together with other by-products that was obtained during FA production. Although other by-products were obtained, FA peak is one of the highest compared to the others.

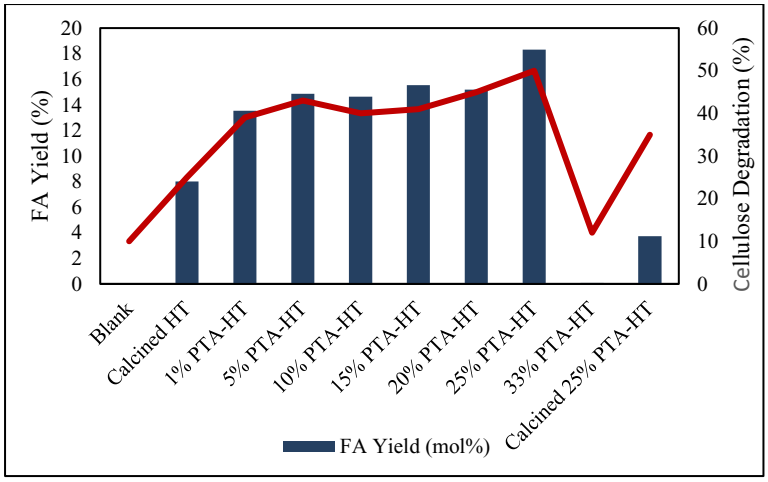

Figure 3. Effect of percentage PTA loading on HT on cellulose conversion and FA yield by PTA-HT catalyst. Reaction condition: 0.05 g cellulose, 0.1 g PTA-HT and temperature at 220 °C

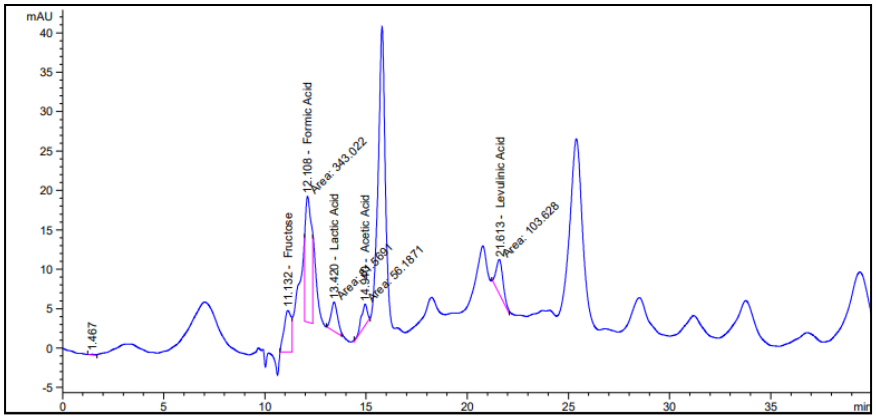

Figure 4. HPLC analysis of cellulose degradation with 0.1g 25% PTA-HT, 4 hours reaction time at 220 ℃

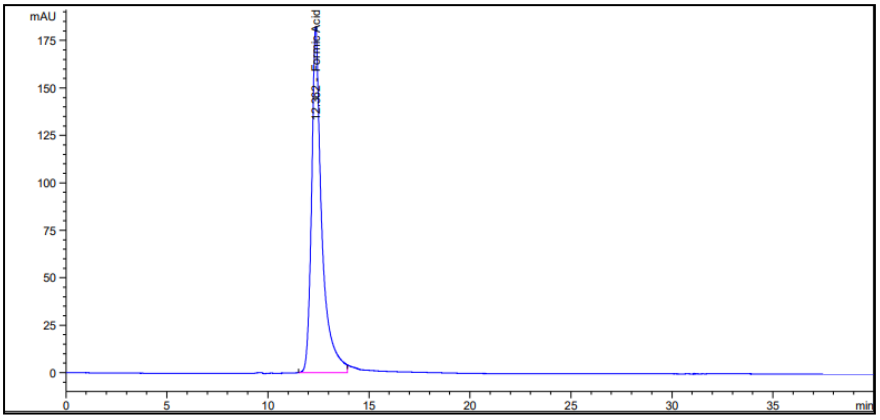

Figure 5. HPLC result for standard FA

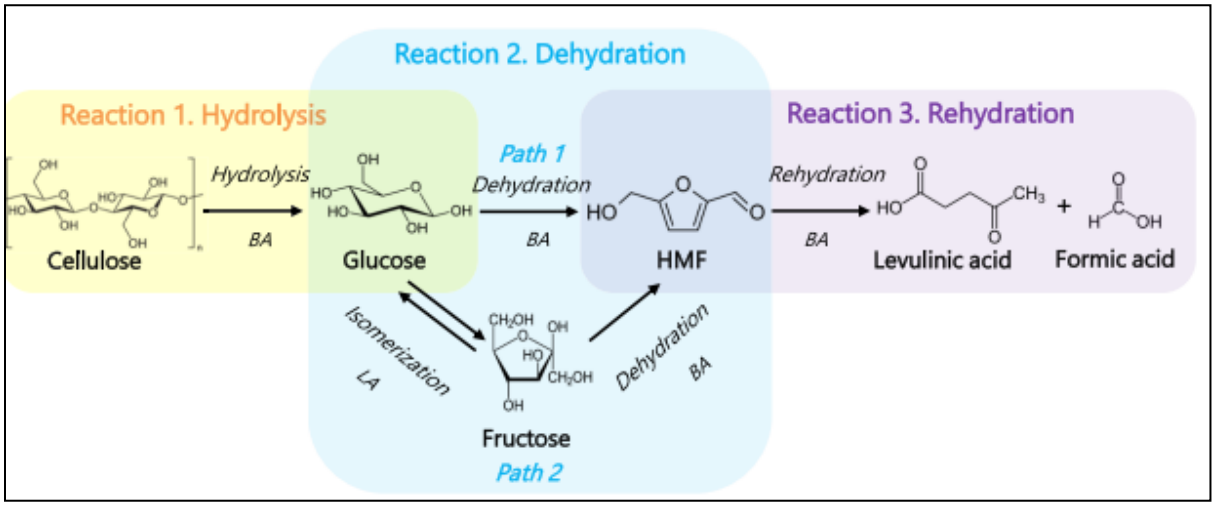

Scheme 1. Mechanism pathway of cellulose degradation into FA [51]

Nitrogen adsorption-desorption analysis

BET measurement has been carried out on raw HT, raw PTA, calcined HT and 25% PTA-HT. The objective of this test is to evaluate the significance of impregnating PTA with calcined HT. One of the drawbacks implementing PTA as homogenous catalyst is because of its low surface area and difficulty to reuse. Hence, having large surface area and porous catalyst support can overcome this. Few journals have reported supported PTA with zirconia, activated carbon and carbon foam but as far as our knowledge there is no PTA supported with calcined HT for cellulose degradation study. As shown in Table 1, raw PTA have the lowest specific surface area as compared to 25% PTA-HT. The main reason to calcined HT is to provide larger surface area and porous surface to support PTA and open more active sites during cellulose degradation. If raw HT was not calcined and impregnated with PTA, we assumed that our catalyst will not be well supported as the surface area for raw HT is small compared to calcined HT. The specific surface area of 25% PTA-HT was significantly lesser than calcined HT is because PTA was deposited inside the pores of calcined HT. Hence, it is important to calcined HT so that the surface area is still larger despite being deposited with PTA.

Table 1. BET analysis of raw HT, calcined HT and 25% PTA-HT

Sample	Specific Surface Area (m^2/g)
Raw HT	10.63
Raw PTA	3.91
Calcined HT	206.62
25% PTA-HT	163.39

XRD analysis

XRD patterns of raw HT (2θ=11.58˚, 23.31˚, 34.42˚, 34.80˚, 35.30˚, 39.32˚, 46.71˚, 52.84˚, 56.32˚, 60.65˚and 61.98˚) and raw PTA (2θ=6.89˚, 8.62˚, 9.33˚, 9.5˚, 10.97˚, 11.66˚, 16.09˚, 17.41˚, 17.83˚, 18.60˚and 19.46˚) showed the typical crystalline structure of Mg-Al layered double hydroxides and phosphotungstic acid respectively. Meanwhile, the XRD peak of calcined HT showed significant difference as crystallinity of raw HT was destructed and formed amorphous mixed oxide phase. This can be seen at 2θ=26.55˚, 29.54˚, 39.52˚ and 62.32˚ that showed an appearance of $MgAl_2O_4$ (spinel) (COD Card No. 5000120). Calcination of HT also gave rise to weak and broad peaks that correlated to MgO known as periclase (COD Card No. 9013246) at 2θ=34.78˚, 43.29˚, 60.70˚ and 79.03˚. As shown in Figure 6, XRD peak of 25 % PTA-HT showed the presence of MgO at 2θ= 38.39˚, $MgAl_2O_4$ (2θ=43.01˚, 62.95˚ and 79.77˚) and (2θ=18.59˚, 28.66˚, 34.79˚ and 47.24˚). This phenomenon is related to calcination of HT that will generate mixed oxide and surface defects. Hence, after calcination of HT at 450 ℃ for 4 hours, original structure of HT lost water and carbonate ions [53]. Removing water and carbonate ions that located at interlayer region will allow incorporation of PTA in MgO framework. Therefore, it is observed that 25% PTA-HT peak follows calcined HT peak. From Figure 4, cellulose peak was observed in sample 25% PTA-HT after reaction because this sample was only separated from liquid product using vacuum filter. Although most peaks appear in 25% PTA-HT after reaction sample, there is missing peak of periclase which might cause from leaching due to reaction condition. However, most of the peaks are maintained in 25% PTA-HT after reaction sample.

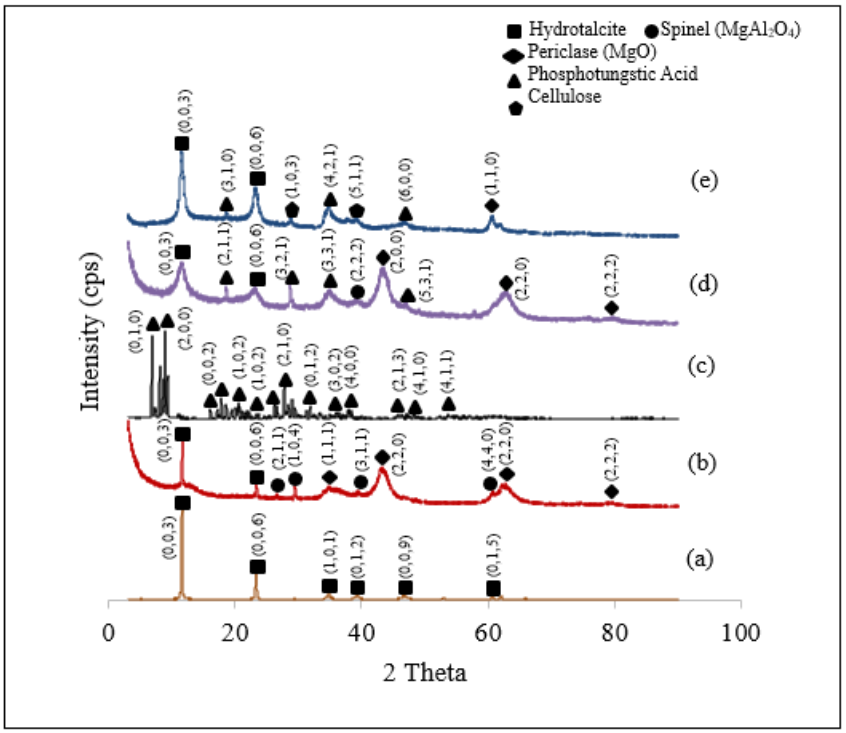

Figure 6. XRD patterns of (a) Raw HT, (b) Calcined HT, (c) Raw PTA, (d) 25% PTA-HT and (e) 25% PTA-HT after reaction

Infrared spectroscopy

IR spectroscopy was used to confirm the presence of PTA after impregnated with calcined HT. As shown in Figure 7, raw PTA was observed to have significant peaks of Keggin HPA at 1071 cm^{-1} (P-O), 970 cm^{-1} (W=O), 899 cm^{-1} (W-O-W) and 729 cm^{-1} (W-O-W) that attributed to stretching vibrational peaks of Keggin anions [54]. The peaks were not obvious because for 25% PTA-HT only 0.025g of PTA impregnated with 0.1g calcined HT. In the case of raw HT, peaks observed at low peaks range between 900-500 cm^{-1} corresponded to metal hydroxides such as $Mg(OH)_2$ and $Al(OH)_3$ [55]. Meanwhile, peaks near 937 cm^{-1} were caused by Mg-O and Al-O. The characteristic peak of raw HT is at 1359 cm^{-1} which is the carbonate and 3403 cm^{-1} for O-H group [56]. The disappearance peaks of metal hydroxides and weak peak of O-H at 3442 cm^{-1} in calcined HT is due to loss of water [57, 58]. IR spectra for 25% PTA-HT, showed the appearances of P-O (1003 cm^{-1}), W=O (801 cm^{-1}), W-O-W (700 cm^{-1}) and Mg-O and Al-O (501 cm^{-1} to 532 cm^{-1}) peaks, which indicated the successful impregnation between PTA and HT. This result can be confirmed with XRD analysis and EDX analysis that can show elements present in the sample.

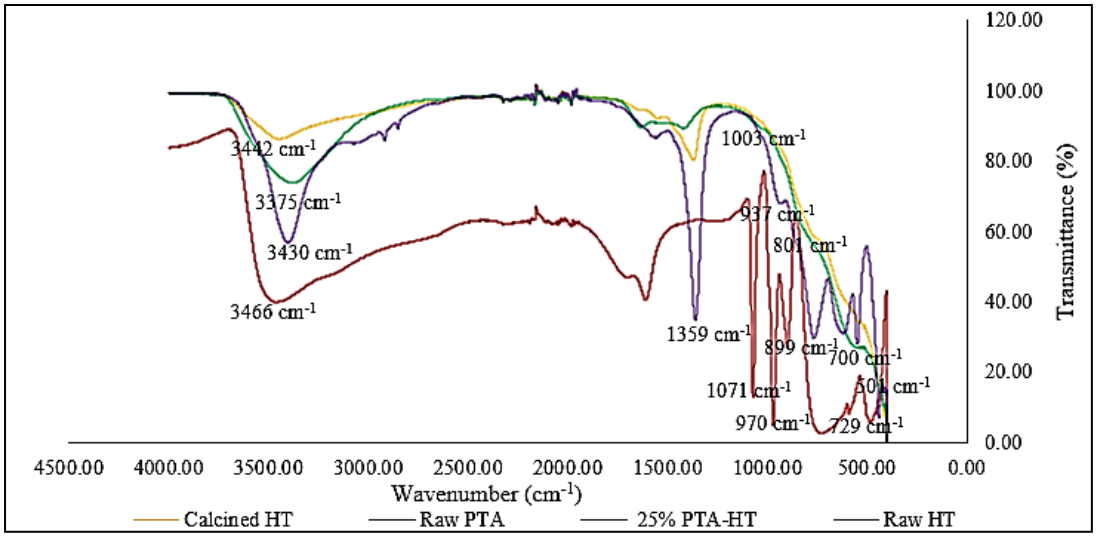

Figure 7. FTIR spectra of raw PTA, raw HT, calcined HT and 25% PTA-HT

FESEM-EDX analysis

FESEM was used to characterize the surface morphology of calcined HT and 25% PTA-HT as shown in Figure 8. Both calcined HT and 25% PTA-HT displayed a similar pattern of particles with irregular shapes. This is because small amount of PTA was impregnated with calcined HT which does not provide any distinguish pattern between calcined HT and 25% PTA-HT. Hence, EDX analysis is important for us to detect the presence of PTA incorporated with calcined HT that can be observed in Figures 9 and 10. As reported before, phosphorus-based HPAs are slightly more acidic than silicon-based HPAs [58]. The importance of tungsten (W) and oxygen (O) inside PTA is their proton affinity which contribute to its acidic site. As shown in Figure 7, the presence of tungsten (W), phosphorus (P) and oxygen (O) indicated the core elements of PTA. Calcination of HT remove carbonate and water at the interlayer and formed mixed oxide where only magnesium (Mg), aluminum (Al) and oxygen were present in Figure 8. The empty interlayer region will be filled with PTA elements and regains its original structure. The unlabeled peaks were carbon tape used for imaging. Both EDX results showed high intensity of Mg, O and Al peaks which shows that calcined HT is more dominant in 25% PTA-HT. Hence, there is no significant difference between FESEM images and FTIR results. Although, calcined HT was dominant the amount of PTA far important towards FA production.

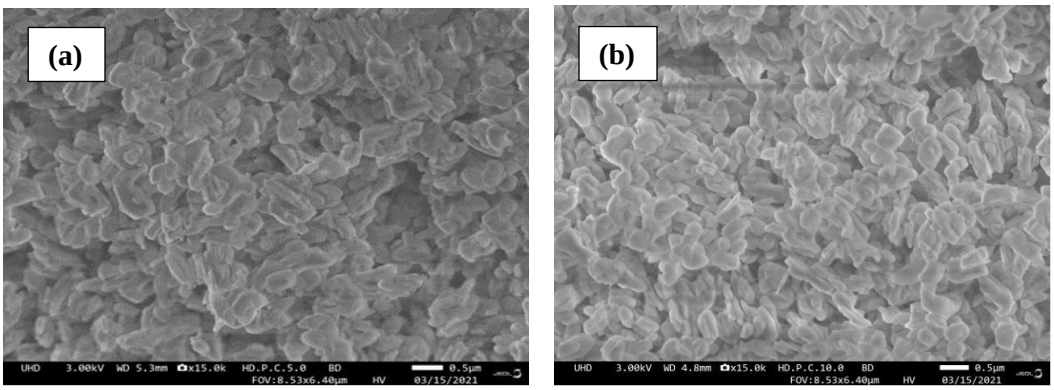

Figure 8. FESEM image of (a) calcined HT and (b) 25% HTA-PTA

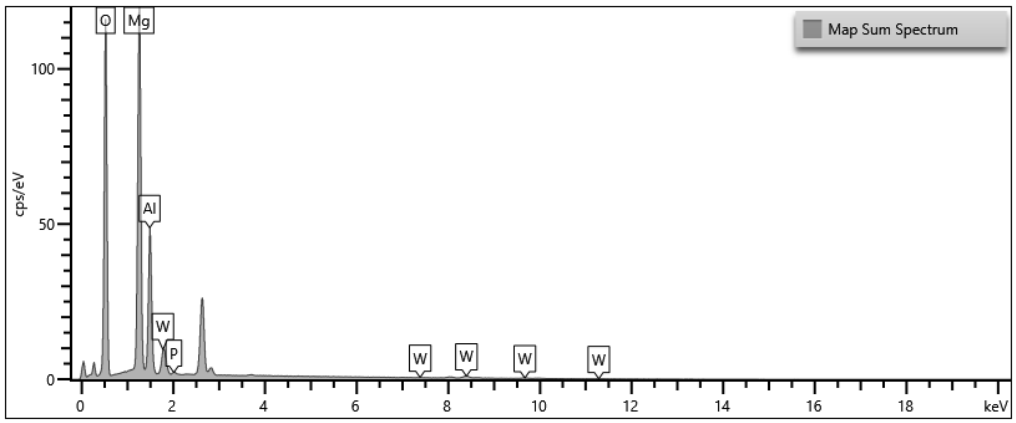

Figure 9. EDX analysis of 25% PTA-HT. Core elements belong to PTA were tungsten (W), phosphorus (P) and oxygen (O). Meanwhile, magnesium (Mg) and aluminum (Al) belong to HT

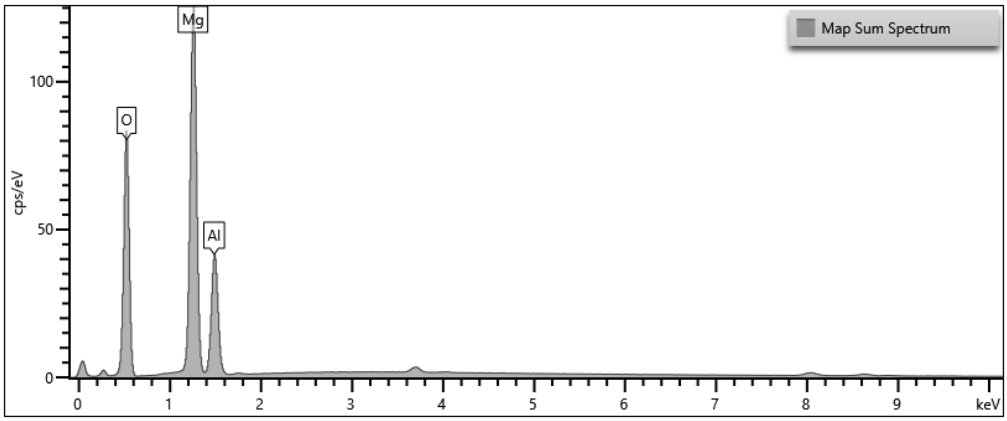

Figure 10. EDX analysis of calcined HT. Core elements belong to calcined HT were magnesium (Mg) and aluminum (Al) belong to HT

Conclusion

From our results, the FA production follows two possible routes contributed by Brönsted acid of PTA and basicity of calcined HT. The basicity of calcined HT may also promote formation of FA while performs well as catalyst support. Although calcined HT is dominant in the catalyst, acidity of PTA plays major role in degrading cellulose into FA. As reported, at optimum condition, 18% FA was yielded together with 30% cellulose degradation which was two times higher than calcined HT alone. To conclude this, the temperature and acidity of catalyst influence the cellulose degradation into FA. However, suitable temperature acidity is required to avoid decomposition of FA. Meanwhile, reaction time have minimal effect towards FA yield. The cellulose degradation can be done independently in water medium but regards to temperature and acid catalyst, the reaction was enhanced. Through catalyst characterization, PTA was successfully impregnated with calcined HT as proved from our results. According to the finding, FA was successfully produced in moderate amounts. Optimum condition for FA yield was as follows: 220℃, 4 hours with 25% catalyst loadings.

Acknowledgement

Authors thank Fundamental Research Scheme Grant (FRGS/1/2019/STG01/USIM/03/1) from Ministry of Education Malaysia for the financial support and Universiti Sains Islam Malaysia for laboratory facilities.

References

1. Foong, S. Y., Liew, R. K., Yang, Y., Cheng, Y. W., Yek, P. N. Y., Mahari, W. A. W., ... and Lam, S. S. (2020). Valorization of biomass waste to engineered activated biochar by microwave pyrolysis: progress, challenges, and future directions. *Chemical Engineering Journal*, 389: 124401.
2. Mamleeva, N. A., Autlov, S. A., Bazarnova, N. G. and Lunin, V. V. (2016). Degradation of polysaccharides and lignin in wood ozonation. *Russian Journal of Bioorganic Chemistry*, 42(7): 694-699.
3. Ribeiro, L. S., de Melo Órfão, J. J. and Pereira, M. F. R. (2017). Simultaneous catalytic conversion of cellulose and corncob xylan under temperature programming for enhanced sorbitol and xylitol production. *Bioresource Technology*, 244: 1173-1177.
4. Scapin, E., Rambo, M. K. D., Viana, G. C. C., Marasca, N., Lacerda, G. E., Rambo, M. C. D. and Fernandes, R. D. M. N. (2019). Sustainable production of furfural and 5-hidroximetilfurfural from rice husks and soybean peel by using ionic liquid. *Food Science and Technology*, 40: 83-87.
5. Dalena, F., Basile, A. and Rossi, C. (Eds.). (2017). *Bioenergy systems for the future: Prospects for biofuels and biohydrogen*. Woodhead Publishing.
6. Tursi, A. (2019). A review on biomass: importance, chemistry, classification, and conversion. *Biofuel Research Journal*, 6(2): 962-979.
7. Nur, N. D., Nur, W. M. Z., Ahmad, H. M., Nor, M. A. and Sheikh, A. I. S. M. G. (2020). Study on the oxidation and properties of dihydroxyl cellulose using different amounts of sodium periodate. *Malaysian Journal of Analytical Sciences*, 24(6): 830-837.
8. Prasad, S. and Ingle, A. P. (2019). Impacts of sustainable biofuels production from biomass. In *Sustainable Bioenergy*, Elsevier. pp. 327-346.
9. Wattanapaphawong, P., Sato, O., Sato, K., Mimura, N., Reubroycharoen, P. and Yamaguchi, A. (2017). Conversion of cellulose to lactic acid by using ZrO_2–Al_2O_3 catalysts. *Catalysts*, *7*(7): 221.
10. Hou, Y., Lin, Z., Niu, M., Ren, S. and Wu, W. (2018). Conversion of cellulose into formic acid by Iron(III)-catalyzed oxidation with O_2 in acidic aqueous solutions. *ACS Omega*, 3(11): 14910-14917.
11. Zhang, M. H., Dong, H., Zhao, L., Wang, D. X. and Meng, D. (2019). A review on Fenton process for organic wastewater treatment based on optimization perspective. *Science of the Total Environment*, 670: 110-121.

12. Morone, A., Mulay, P. and Kamble, S. P. (2019). Removal of pharmaceutical and personal care products from wastewater using advanced materials. *Pharmaceuticals and Personal Care Products: Waste Management and Treatment Technology*, 2019: 173-212.
13. Ma, J., Zhang, K., Huang, M., Hector, S. B., Liu, B., Tong, C., ... and Zhu, Y. (2016). Involvement of Fenton chemistry in rice straw degradation by the lignocellulolytic bacterium *Pantoea ananatis* Sd-1. *Biotechnology for Biofuels*, 9(1): 1-13.
14. Awudu, F. (2018). Hydrolysis of Cellulose and Biomass using Blue Molybdenum (Doctoral dissertation, East Tennessee State University).
15. Gromov, N. V., Medvedeva, T. B., Rodikova, Y. A., Babushkin, D. E., Panchenko, V. N., Timofeeva, M. N., ... and Parmon, V. N. (2020). One-pot synthesis of formic acid via hydrolysis–oxidation of potato starch in the presence of cesium salts of heteropoly acid catalysts. *RSC Advances*, 10(48): 28856-28864.
16. Cheng, C., Wang, J., Shen, D., Xue, J., Guan, S., Gu, S. and Luo, K. H. (2017). Catalytic oxidation of lignin in solvent systems for production of renewable chemicals: A review. *Polymers*, 9(6): 240.
17. Albert, J. (2017). Selective oxidation of lignocellulosic biomass to formic acid and high-grade cellulose using tailor-made polyoxometalate catalysts. *Faraday Discussions*, 202: 99-109.
18. Chen, X., Liu, Y. and Wu, J. (2020). Sustainable production of formic acid from biomass and carbon dioxide. *Molecular Catalysis*, 483: 110716.
19. Voß, D., Dietrich, R., Stuckart, M. and Albert, J. (2020). Switchable catalytic polyoxometalate-based systems for biomass conversion to carboxylic acids. *ACS Omega*, *5*(30), 19082-19091.
20. Doungsri, S., Rattanaphanee, P. and Wongkoblap, A. (2019). Production of lactic acid from cellulose using solid catalyst. In *MATEC Web of Conferences*, 268: 07006).
21. Sun, Y., Shi, L., Wang, H., Miao, G., Kong, L., Li, S. and Sun, Y. (2019). Efficient production of lactic acid from sugars over Sn-Beta zeolite in water: catalytic performance and mechanistic insights. Sustainable *Energy & Fuels*, 3(5): 1163-1171.
22. Ramli, N. A. S. and Amin, N. A. S. (2015). Fe/HY zeolite as an effective catalyst for levulinic acid production from glucose: characterization and catalytic performance. *Applied Catalysis B: Environmental*, 163: 487-498.
23. Bhorodwaj, S. K. and Dutta, D. K. (2011). Activated clay supported heteropoly acid catalysts for esterification of acetic acid with butanol. *Applied Clay Science*, 53(2): 347-352.
24. Hietala, J., Vuori, A., Johnsson, P., Pollari, I., Reutemann, W. and Kieczka, H. (2016). Formic acid. *Ullmann's Encyclopedia of Industrial Chemistry*, 1: 1-22.
25. Ricke, S. C., Dittoe, D. K. and Richardson, K. E. (2020). Formic acid as an antimicrobial for poultry production: A review. *Frontiers in Veterinary Science*, 2020: 563.
26. Johnson Jr, W., Heldreth, B., Bergfeld, W. F., Belsito, D. V., Hill, R. A., Klaassen, C. D., ... and Andersen, F. A. (2016). Safety assessment of formic acid and sodium formate as used in cosmetics. *International Journal of Toxicology*, 35(2): 41S-54S.
27. Kos, L., Michalska, K., Żyłła, R. and Perkowski, J. (2014). Effect of formic acid on pollutant decomposition in textile wastewater subjected to treatment by the Fenton method. *Fibres & Textiles in Eastern Europe*, 22, 135-139.
28. del Barrio, M. A., Hu, J., Zhou, P. and Cauchon, N. (2006). Simultaneous determination of formic acid and formaldehyde in pharmaceutical excipients using headspace GC/MS. *Journal of Pharmaceutical and Biomedical Analysis*, 41(3): 738-743.
29. Higgins, F. J. and Ho, G. E. (1982). Hydrolysis of cellulose using HCl: a comparison between liquid phase and gaseous phase processes. *Agricultural Wastes*, 4(2): 97-116.
30. Goldstein, I. S., Pereira, H., Pittman, J. L., Strouse, B. A. and Scaringelli, F. P. (1983, January). Hydrolysis of cellulose with superconcentrated hydrochloric acid. In *Biotechnol. Bioeng. Symp.;(United States)*, 13: No. CONF-830567. North Carolina State Univ., Raleigh.

31. Dussán, K. J., Silva, D. D., Moraes, E. J., Arruda, P. V. and Felipe, M. G. (2014). Dilute-acid hydrolysis of cellulose to glucose from sugarcane bagasse. *Chemical Engineering Transaction*, 38: 433-438.
32. Alcañiz-Monge, J., El Bakkali, B., Trautwein, G. and Reinoso, S. (2018). Zirconia-supported tungstophosphoric heteropolyacid as heterogeneous acid catalyst for biodiesel production. *Applied Catalysis B: Environmental*, 224: 194-203.
33. Anggorowati, H., Jamilatun, S., Cahyono, R. B. and Budiman, A. (2018). Effect of hydrochloric acid concentration on the conversion of sugarcane bagasse to levulinic acid. In *IOP Conference Series: Materials Science and Engineering*, 299(1): p. 012092.
34. Huang, P. and Yan, L. F. (2017). Efficient degradation of cellulose in its homogeneously aqueous solution over 3D metal-organic framework/graphene hydrogel catalyst. *Chinese Journal of Chemical Physics*, 29(6): 742.
35. Sivasubramaniam, D., Amin, N. A. S., Ahmad, K. and Ramli, N. A. S. (2019). Production of ethyl levulinate via esterification reaction of levulinic acid in the presence of ZrO_2 based catalyst. *Malaysian Journal of Analytical Sciences*, 23(1): 45-51.
36. Demesa, A. G., Laari, A., Sillanpää, M. and Koiranen, T. (2017). Valorization of lignin by partial wet oxidation using sustainable heteropoly acid catalysts. *Molecules*, 22(10): 1625.
37. Zhang, Z., Wang, B., Zhang, Y., Zhang, G. and Wang, Y. (2019). Study on the synthesize, characterization, and conductive performance of nickelzircomolybdnum heteropoly acid salt with Keggin structure. *Advances in Polymer Technology*, 2019: 501593.
38. Guarin, C., Gavila, L., Constanti, M. and Medina, F. (2018). Impact of cellulose treatment with hydrotalcites in hydrothermal catalytic conversion. *Chemical Engineering Science*, 179: 83-91.
39. Ziyat, H., Naciri Bennani, M., Hajjaj, H., Mekdad, S. and Qabaqous, O. (2018). Synthesis and characterization of crude hydrotalcite Mg–Al–CO_3: study of thymol adsorption. *Research on Chemical Intermediates*, 44(7): 4163-4177.
40. Li, T., Miras, H. N. and Song, Y. F. (2017). Polyoxometalate (POM)-layered double hydroxides (LDH) composite materials: design and catalytic applications. *Catalysts*, 7(9): 260.
41. Omwoma, S., Chen, W., Tsunashima, R. and Song, Y. F. (2014). Recent advances on polyoxometalates intercalated layered double hydroxides: From synthetic approaches to functional material applications. *Coordination Chemistry Reviews*, 258: 58-71.
42. Sasaki, M., Fang, Z., Fukushima, Y., Adschiri, T. and Arai, K. (2000). Dissolution and hydrolysis of cellulose in subcritical and supercritical water. *Industrial & Engineering Chemistry Research*, 39(8): 2883-2890.
43. Paksung, N., Pfersich, J., Arauzo, P. J., Jung, D. and Kruse, A. (2020). Structural effects of cellulose on hydrolysis and carbonization behavior during hydrothermal treatment. *ACS Omega*, 5(21): 12210-12223.
44. De Guzman, D. and De Leon, R. (2021). Preliminary optimization and kinetics of $SnCl_2$-HCl catalyzed hydrothermal conversion of microcrystalline cellulose to Levulinic acid. *Journal of Renewable Materials*, 9(1): 145.
45. Wang, K., Liu, Y., Wu, W., Chen, Y., Fang, L., Li, W. and Ji, H. (2020). Production of levulinic acid via cellulose conversion over metal oxide-loaded MOF catalysts in aqueous medium. *Catalysis Letters*, 150(2): 322-331.
46. Li, X., Lu, X., Nie, S., Liang, M., Yu, Z., Duan, B., ... and Si, C. (2020). Efficient catalytic production of biomass-derived levulinic acid over phosphotungstic acid in deep eutectic solvent. *Industrial Crops and Products*, 145: 112154.
47. Lauermannová, A. M., Paterová, I., Patera, J., Skrbek, K., Jankovský, O. and Bartůněk, V. (2020). Hydrotalcites in construction materials. *Applied Sciences*, 10(22): 7989.

48. Gromov, N. V., Taran, O. P., Delidovich, I. V., Pestunov, A. V., Rodikova, Y. A., Yatsenko, D. A., ... and Parmon, V. N. (2016). Hydrolytic oxidation of cellulose to formic acid in the presence of Mo-VP heteropoly acid catalysts. *Catalysis Today*, 278: 74-81.
49. Guarin, C., Gavila, L., Constanti, M. and Medina, F. (2018). Impact of cellulose treatment with hydrotalcites in hydrothermal catalytic conversion. *Chemical Engineering Science*, 179: 83-91.
50. Delidovich, I. and Palkovits, R. (2015). Structure–performance correlations of Mg–Al hydrotalcite catalysts for the isomerization of glucose into fructose. *Journal of Catalysis*, 327: 1-9.
51. Tulaphol, S., Hossain, M. A., Rahaman, M. S., Liu, L. Y., Phung, T. K., Renneckar, S., ... and Sathitsuksanoh, N. (2019). Direct production of levulinic acid in one pot from hemp hurd by dilute acid in ionic liquids. *Energy & Fuels*, 34(2): 1764-1772.
52. Dandach, A., Vu, T. T. H., Fongarland, P. and Essayem, N. (2019). ZrW catalyzed cellulose conversion in hydrothermal conditions: Influence of the calcination temperature and insights on the nature of the active phase. *Molecular Catalysis*, 476: 110518.
53. Tian, J., Wang, J., Zhao, S., Jiang, C., Zhang, X. and Wang, X. (2010). Hydrolysis of cellulose by the heteropoly acid $H_3PW_{12}O_{40}$. *Cellulose*, 17(3): 587-594.
54. Xiaohua, C., Jie, R., Changlong, X., Zhang, K., Changchao, Z. H. A. N., and Jian, L. A. N. (2013). Preparation, characterization of Dawson-type heteropoly acid cerium (III) salt and its catalytic performance on the synthesis of n-butyl acetate. *Chinese Journal of Chemical Engineering*, 21(5): 500-506.
55. Julianti, N. K., Wardani, T. K., Gunardi, I. and Roesyadi, A. (2017). Effect of calcination at synthesis of Mg-Al hydrotalcite using co-precipitation method. *The Journal of Pure and Applied Chemistry Research*, 6(1): 7.
56. Jia, Y., Fang, Y., Zhang, Y., Miras, H. N. and Song, Y. F. (2015). Classical Keggin intercalated into layered double hydroxides: facile preparation and catalytic efficiency in Knoevenagel condensation reactions. *Chemistry–A European Journal*, 21(42): 14862-14870.
57. Liu, G., Yang, J. and Xu, X. (2020). Synthesis of hydrotalcite-type mixed oxide catalysts from waste steel slag for transesterification of glycerol and dimethyl carbonate. *Scientific Reports*, 10(1): 1-14.
58. Roohollahi, G. and Ehsani, M. (2019). An investigation into the effect of hydrotalcite calcination temperature on the catalytic performance of mesoporous Ni-MgO-Al_2O_3 catalyst in the combined steam and dry reforming of methane. *Iranian Journal of Oil and Gas Science and Technology*, 8(4): 64-84.
59. Bardin, B. B., Bordavekar, S. V., Neurock, M. and Davis, R. I. (1998). Analysis of kegging-type heteropoly compounds evaluated by catalytic probe reaction sorption microcalorimetry and density functional quantum chemical calculations. *Journal Physical Chemistry*, 102: 10817-10825.